High-Energy Proton Spallation-Fission of Uranium

R. L. FOLGER,* P. C. STEVENSON, AND G. T. SEABORG
Radiation Laboratory and Department of Chemistry, University of California, Berkeley, California
(Received November 12, 1954)

The fission and spallation reactions produced in uranium by bombardment with high-energy protons (340 to 350 Mev) were investigated. The reaction products were separated from the target by chemical processes and identified by their radioactive properties. The relative yields of the observed fission products are calculated, and the results plotted as a function of mass number. Several of the spallation products are identified and their yields estimated.

An attempt is made to determine the most probable atomic number for a nuclide of given mass formed directly from fission. Studies are made of the relative yields along several isobaric chains as a function of atomic number. From these data, estimates of the mass and charge of the fissioning nucleus are made.

By using the reaction $Al^{27}(p,3pn)Na^{24}$ of known cross section to monitor the bombarding beam, the absolute formation cross sections for several fission product nuclides were measured. Values for these reference nuclides are used to transform all of the relative yields into formation cross sections. Summation integration over the range of mass numbers of the area under the plot of formation cross sections as a function of mass number leads to a value of 2.0 barns for the total fission cross section for uranium bombarded with high-energy protons, if one assumes binary fission.

I. INTRODUCTION

IN recent years there has been considerable interest in the mechanism of fission induced by high-energy particles (greater than a few Mev) as compared to that of low-excitation fission. This work has been reviewed by Spence and Ford.[1] In the case of the heavy elements, work has been done with the target elements bismuth,[2–4] thorium,[4–8] and uranium.[4,9–11] High-energy fission of tantalum[12] and other heavy elements[2] from $Z=73$ to $Z=82$ has been observed. Batzel and Seaborg[13] have announced the high-energy fission of a number of medium weight elements. The yield distribution of fission products has been studied by chemical separation techniques followed by identification of the nuclides through radioactivity measurements, and also by measurement of the kinetic energies of the fission fragments.

The predominant characteristics of very high-energy fission which appear from these studies are:

(1) A single peak is found in the yield *versus* mass distribution curve, as opposed to the double peak found in low-energy fission.

(2) Prefission evaporation of nucleons is suggested. The mass number of the peak of the yield distribution is substantially less than one-half the mass number of the target nucleus.

(3) The kinetic energies of the fission fragments seem to be practically independent of the initial target-nucleus excitation.[4,14]

Predominantly symmetric fission caused by very high-energy particles has been reported by Goeckermann and Perlman[2] (bismuth plus 190-Mev deuterons), Biller and Perlman[3] (bismuth plus 340-Mev protons), O'Connor and Seaborg[9] (uranium plus 380-Mev helium ions), and Jungerman and Wright[4] (uranium plus 90-Mev neutrons).[15] At intermediate energies, the contribution of asymmetric fission is shown by the appearance of two peaks with a shallow dip between them with the peak-to-trough ratio increasing as the energy is decreased. This effect has been observed by Newton[5] (thorium plus 38-Mev helium ions), Jungerman and Wright[4] (uranium plus 45-Mev neutrons), Tewes and James[6] (thorium plus 6.7- to 21.1-Mev protons), Fowler, Jones, and Paehler[11] (uranium plus 11- to 18-Mev protons), Turkevich and Niday[7] (thorium plus pile neutrons), Turkevich, Niday, and Tompkins[8] (thorium plus 6- to 11-Mev neutrons) and Spence[16] (U^{235} plus 14, $\sim$1.2, and $\sim$0.4 Mev neutrons). The same effect has been observed in photofission by Schmitt and Sugarman[17] (uranium plus 7 to 300 Mev x-rays), Hiller and Martin[18] (thorium plus 69-Mev

* Now at E. I. du Pont de Nemours Company, Savannah River Plant, Augusta, Georgia.

[1] R. W. Spence and G. P. Ford, Ann. Rev. Nuc. Sci. **2**, 399 (1953).

[2] R. H. Goeckermann and I. Perlman, Phys. Rev. **73**, 1127 (1948); **76**, 628 (1949); Perlman, Goeckermann, Templeton, and Howland, **72**, 352 (1947).

[3] W. F. Biller and I. Perlman (unpublished); W. F. Biller, Ph.D thesis, University of California, Berkeley, California (unpublished).

[4] J. Jungerman and S. C. Wright, Phys. Rev. **76**, 1112 (1949).

[5] A. S. Newton, Phys. Rev. **75**, 17 (1949).

[6] H. A. Tewes and R. A. James, Phys. Rev. **88**, 860 (1952).

[7] A. Turkevich and J. B. Niday, Phys. Rev. **84**, 52 (1951).

[8] Turkevich, Niday, and Tompkins, Phys. Rev. **89**, 552 (1953).

[9] P. R. O'Connor and G. T. Seaborg, Phys. Rev. **74**, 1189 (1948).

[10] M. Lindner and R. Osborne, Phys. Rev. **94**, 1323 (1954).

[11] Fowler, Jones, and Paehler, Phys. Rev. **88**, 7 (1952).

[12] W. Nervik and G. T. Seaborg, Phys. Rev. **97**, 1092 (1955).

[13] R. E. Batzel and G. T. Seaborg, Phys. Rev. **79**, 528 (1950); Phys. Rev. **82**, 607 (1951). See also D. H. Greenberg and J. M. Miller, Phys. Rev. **84**, 845 (1951) and P. K. Kofstad, Ph.D. thesis, University of California Radiation Laboratory Report UCRL-2265, June, 1953 (unpublished).

[14] E. M. Douthett and D. H. Templeton, Phys. Rev. **94**, 128 (1954).

[15] Represents ionization chamber measurement of fragment kinetic energies.

[16] R. W. Spence, Brookhaven National Laboratory BNL-C-9, June, 1949 (unpublished), p. 43.

[17] R. A. Schmitt and N. Sugarman, Phys. Rev. **95**, 1260 (1954).

[18] D. M. Hiller and D. S. Martin, Jr., Phys. Rev. **90**, 581 (1953).

x-rays), Spence[16] (U^{235} plus 12 to 16-Mev x-rays), and Richter and Coryell[19] (uranium plus 9- to 14-Mev x-rays).

Recent results at extremely high energies, 2-Bev protons on lead[20] and bismuth,[21] show mass number distribution curves unlike those observed in the hundred-Mev range, with a monotonic decrease in yield with decreasing atomic numbers of the product throughout the entire range of the products. It appears that more work at these extremely high and at intermediate energies will be necessary before these results can be correlated with results such as those presented here from investigations in the hundred-Mev range.

In the high-energy (190-Mev) deuteron fission of bismuth, Goeckermann and Perlman[2] observed that the mass number at the symmetric peak of the fission-product distribution curve was less than one-half the mass number of the target nucleus. The mass difference indicated the evaporation of 10 to 12 nucleons. The relative yields of the fission-product isobars seemed to indicate that the most probable primary products were those having the same charge-to-mass ratio as the fissioning nucleus. Yamaguchi,[22] in a theoretical treatment of nuclear evaporation, has indicated that for bismuth bombarded with 200-Mev deuterons, the probability for neutron emission may be greater than that for fission until 10 to 11 neutrons have been emitted. In the case of uranium bombarded with 380-Mev helium ions,[9] the mass number at the peak of the distribution curve was not well enough defined to demonstrate corresponding neutron emission although the curve showed a strong possibility that such evaporation had occurred.

Measurements of fission-fragment kinetic energies have been made by Jungerman and Wright,[4] using ionization chamber techniques, and indirectly by Douthett and Templeton,[14] who measured the ranges of the fragments in aluminum. In bombarding uranium with 45- and 90-Mev neutrons, Jungerman and Wright[4] observed the mean kinetic energies to be 79 ± 3 and 80 ± 2 Mev, respectively. Within the limits of experimental error, the ranges of fission fragments obtained by radiochemical separation from absorber foils are equal for the corresponding products formed by slow-neutron fission of U^{235},[23,24] uranium plus 18-Mev deuterons,[14] and uranium plus 335-Mev protons,[14] if one takes account of the changes in mass of the complementary fragments. These results seem to indicate that there is no mechanism for converting excitation energy into recoil energy. The excitation energy goes into the emission of nucleons, mostly neutrons, but the information presently available is not sufficient to allow a decision as to whether the neutrons are emitted before or after the separation of the nucleus into the primary fission fragments. The results are consistent with the picture in which the actual fissioning nucleus in each case is in a relatively unexcited state following the dissipation of the initial excitation energy primarily by the prefission evaporation of nucleons.

II. EXPERIMENTAL PROCEDURES

Our work has been done by bombarding uranium in the circulating proton beam of the 184-in. Berkeley cyclotron. The proton energy at the radius used is approximately 340 Mev. The fission products so produced were isolated by standard radiochemical means and identified by observation of their half-lives and radiation characteristics. In the early work it was customary to evaporate an aliquot of the final solution on a counting plate for the radioactive sample, then precipitate a suitable compound for the gravimetric analysis from the balance of the solution. In later work it was found desirable to use the final precipitate itself, after weighing, for the radioactive sample (see sections below on scattering and absorption corrections). In these cases the final precipitate, after washing, was slurried with an organic liquid and transferred by pipet to an aluminum dish approximately one inch in diameter and weighing between 70 and 80 mg. The sensitivity of the balance used was of the order of 10^{-2} mg and the sample usually had a net weight between 1 and 10 mg. In contrast to samples dried and weighed on filter paper, samples mounted on aluminum dishes show much greater weight stability since the aluminum does not absorb moisture from the air.

Detecting instruments.—Alpha-emitting samples were measured either in a proportional counter or in an ionization chamber instrument. Alpha energies were determined by means of an alpha pulse analyzer.[25]

Samples emitting beta and gamma radiation were counted by means of end-window Geiger-Müller tubes. When this work was begun, the tubes available were of the argon-alcohol type. For the more recent work, end-window tubes filled with a mixture of argon and chlorine were used. These tubes (Amperex Type 100C, obtainable from Amperex Electronic Company, New York, New York) have a window thickness of 3.5 mg/cm^2.

Backscattering.—Correction factors for the scattering of beta particles into the counter from the backing material on which the sample is mounted have been empirically determined by several workers.[26–28] The

[19] H. G. Richter and C. D. Coryell, Phys. Rev. **95**, 1550 (1954).
[20] J. M. Miller and G. Friedlander, Phys. Rev. **91**, 485 (1953).
[21] Sugarman, Duffield, Friedlander, and Miller, Phys. Rev. **95**, 1704 (1954).
[22] Y. Yamaguchi, Progr. Theoret. Phys. (Japan) **5**, 143 (1950).
[23] Finkle, Hoagland, Katcoff, and Sugarman, *Radiochemical Studies: The Fission Products* (McGraw-Hill Book Company, Inc., New York, 1951), paper No. 46, National Nuclear Energy Series, Plutonium Project Record, Vol. 9B.
[24] F. Suzor, Ann. Physik **124**, 269 (1949).
[25] Ghiorso, Jaffey, Robinson, and Weissbourd, *The Transuranium Elements: Research Papers* (McGraw-Hill Book Company, Inc., New York, 1949), paper No. 16.8, National Nuclear Energy Series, Plutonium Project Record, Vol. 14B.
[26] L. R. Zumwalt, U. S. Atomic Energy Commission Declassified Document MDDC-1346, Februrary, 1949 (unpublished).
[27] B. P. Burtt, Nucleonics **5**, No. 2, 28 (1949).

amount of backscatter depends primarily upon the thickness and atomic number of the backing material. The scattering is relatively insensitive to beta energy in the range 0.6 to 3 Mev.[27,28] In most of our work, the samples were mounted on similar backings so that for relative yields the backscattering correction nearly cancelled out for all but soft beta particles.

Self-scattering and self-absorption corrections.—Since the radioactive samples in many cases were of finite mass, it was necessary to determine the loss or gain of apparent activity in passing through the mass of the sample. There is a loss of apparent activity due to absorption in the material of the sample. Scattering of beta particles and electrons by the material of the sample causes an apparent increase in the activity. Some preliminary experiments were performed to determine empirically the combined self-absorption and self-scattering corrections.[29,30] The absorbing power of sample material for particles increases only slowly with the atomic number, but the scattering power increases markedly. In some cases the scattering effects were so great that a net increase in apparent counting rate was obtained even for many milligrams per square centimeter of sample thickness. Uncertainties in the self-scattering corrections are believed to be the major source of error in our measurements.

Air-window absorption.—The loss of activity by absorption in the air between the sample and the counter window, and in the window itself, was determined by extrapolation of aluminum and/or beryllium absorption curves whose initial portions were carefully measured by using thin absorbers.

Counting efficiencies.—In determining yields of various nuclides, it was necessary to make some assumptions regarding relative counting efficiencies. For beta particles and electrons a counting efficiency of 100 percent was assumed. The calculated counting efficiencies for electromagnetic radiation, based on absorption in the gas of the counter tube, were 0.5 percent for energies from 20 kev to 0.5 Mev, and 1 percent per Mev thereafter for argon-filled tubes.[31] The ratio of the over-all efficiency of the argon-chlorine (Amperex) tubes to the argon-alcohol tubes for the same geometrical arrangement was determined to be 45 percent by counting a number of samples having beta and electromagnetic radiations of various energies.[32]

Effective geometry.—The sample holders used for the counting with the Geiger-Müller tubes could be placed in any one of five positions varying from 0.3 to 6.7 cm from the tube window. Attempts were usually made to measure the counting rate with a monitor sample in the same position as the sample of the nuclide whose relative yield was being determined. When such an arrangement was not practical initially because of too great a difference in the counting rates of the samples, the "geometry" ratio was later determined empirically when the counting rates were more nearly equal. This ratio was not a true geometric ratio alone because of increased air absorption at greater distances from the counter window. In cases where the absorption characteristics of a particular beta particle were rather well known, measurements of the true geometric ratios between various positions were made.

III. ACTIVE SPECIES OBSERVED

Sodium.—The isolated sodium fraction from a uranium target, prepared with extreme care to eliminate any light-element surface contamination, showed a beta activity of 15-hour half-life in amount larger than could be accounted for by impurities in the uranium. The decay was followed for four half-lives without any deviation because of radioactive impurities being observed. Aluminum absorption measurements of the beta radiation showed the 1.4-Mev beta particle of Na^{24}.[33–35]

Manganese.—A 5.8-day activity was observed in the manganese fraction separated after an eight-hour bombardment of a uranium target. The absorption characteristics and half-life corresponded to those observed for Mn^{52} formed by spallation of iron with 340-Mev protons. The amount of Mn^{52} produced could be accounted for by the known amounts of iron and nickel impurities in the uranium target. No manganese activity was observed which could unambiguously be attributed to uranium fission.

Iron.—The iron fraction decay showed two major components. One was the expected 46-day Fe^{59}, characterized by half-life and aluminum absorption measurements. The other component had a half-life of approximately 8 hours and very energetic negative beta radiations. This was at first thought to be a new isotope of iron, but is now believed to be caused by gallium contamination, the observed half-life being caused by a mixture of Ga^{72} and Ga^{73}.

Cobalt.—Decay measurements of the cobalt fraction showed a component of 1.7 hours, corresponding to Co^{61}. Aluminum absorption measurements of the 1.7-hour activity showed a beta energy of about 1.3 Mev.

Nickel.—The decay of nickel showed components of 2.6 hours and 56 hours, corresponding to Ni^{65} and Ni^{66}, respectively. Aluminum absorption measurements of the 56-hour Ni^{66} showed the 2.9-Mev beta particle of 4.3-minute Cu^{66} in equilibrium.

---

[28] L. Yaffe and K. M. Justus, J. Chem. Soc. (London) 341 (1949).
[29] L. Malatesta (unpublished).
[30] W. Nervik and P. C. Stevenson, Nucleonics **10**, No. 3, 18 (1952).
[31] M. Studier and R. James (unpublished).
[32] E. Potter and H. P. Robinson (unpublished).
[33] Unless otherwise indicated, values of the half-life and beta-particle energy for the various nuclides were obtained from either the *Table of Isotopes* or the *Chart of the Nuclides*.
[34] Hollander, Perlman, and Seaborg, Revs. Modern Phys. **25**, 469 (1953).
[35] General Electric Chart of the Nuclides, Knolls Atomic Power Laboratory, Fourth Edition, originally prepared by G. Friedlander and M. Perlman, revised by J. R. Stehn.

Copper.—Three isotopes of copper were identified. The 3.4-hour Cu^{61} was observed by following the decay of its positrons with a crude beta ray spectrometer. The 12.9-hour Cu^{64} was also seen in this manner as well as by resolution of the decay curve obtained with a conventional Geiger-Müller counter. Sixty-hour Cu^{67} was clearly seen as a component in the beta decay curve.

Fermi-Kurie plots of the crude beta-spectrometer positron data showed the 1.2-Mev β^+ of Cu^{61} and the 0.66-Mev β^+ of Cu^{64}. Aluminum absorption measurements, taken after the 12.9-hour activity had decayed, showed the 0.6-Mev β^- of Cu^{67}. Careful spectrographic analyses of the uranium revealed that sufficient zinc, copper, and nickel impurities were present to give the observed yields of the neutron-deficient copper isotopes. The correction to the Cu^{67} yield from this source is small.

Zinc.—Observation of the decay of the zinc samples showed a half-life of 49 hours. A growth corresponding to a daughter half-life of 14 hours was observed, indicating the presence of 49-hour Zn^{72} with 14-hour Ga^{72} daughter.

Arsenic.—Decay of the arsenic radiation observed through 350 mg/cm^2 of aluminum (to block the particulate radiation of As^{77}) showed an activity of 26.8-hour half-life, corresponding to As^{76}. Observations without absorber showed the 40-hour activity of As^{77}.

Selenium.—The predominant activity in the selenium samples was the 59-minute Se^{81m} with the 17-minute Se^{81} in equilibrium. It was possible to detect the 25-minute Se^{83} both by resolution of the decay curve and by observing the 2.4-hour Br^{83} daughter in the decay measurements. Twenty-four hours after bombardment, the decay curve showed essentially no activity other than the 2.4-hour Br^{83}.

Aluminum absorption measurements on the 59-minute activity showed the 1.5-Mev beta particle of Se^{81}.

Bromine.—The bromine decay curves showed mainly 2.4-hour and 35-hour components when measurements were made without absorber. Decay of radiation measured through 490 mg/cm^2 of aluminum showed components of 4.4-hour and of 34-minute half-lives after subtraction of a 35-hour component due to the penetrating radiation of Br^{82}. Measurements through 750 mg/cm^2 of aluminum showed a component of 34-minute half-life and a residuum of 4.4-hour and 35-hour activities. The relative counting efficiency for the 4.4-hour activity was considerably reduced by the increased absorber. Aluminum absorption measurements of the 2.4-hour activity showed a 1-Mev beta particle.

From the evidence we conclude that Br^{80m}, Br^{82}, Br^{83}, and Br^{84} are formed as fission products with Br^{83} being produced in highest yield.

Rubidium.—The rubidium sample showed an activity of 19.5-day half-life, corresponding to Rb^{86}. The sample was not isolated soon enough to detect any of the shorter-lived rubidium isotopes. Aluminum absorption measurements on the rubidium activity showed a 1.8-Mev beta particle.

Strontium.—From decay measurements a 9.7-hour strontium activity was observed. A 60-day yttrium activity was chemically separated from the strontium sample, indicating the presence of Sr^{91}. Another strontium sample, from which yttrium had been removed a week after bombardment of the target, showed an activity of 54-day half-life. Aluminum absorption measurements on the 54-day activity showed the presence of the characteristic 1.5-Mev beta particle of Sr^{89}. The background due to electromagnetic radiation was negligible.

Zirconium.—The zirconium decay showed a 17-hour activity from which grew a 69-minute daughter, indicating the presence of Zr^{97} and Nb^{97}. After decay of the Zr^{97}, a decay line of predominantly 65 days half-life (Zr^{95}) was seen.

Niobium.—Four major species were identified in the niobium decay: 68-minute Nb^{97}; an activity of approximately 23 hours, probably Nb^{96}; 90-hour Nb^{95m} as established by analytical treatment of the counting data; and 37-day Nb^{95}.

Molybdenum.—The only activity observed in the molybdenum fraction was the 67-hour Mo^{99}. Activities of less than 30-minute half-life would not have been observed.

Ruthenium.—Decay measurement showed a 4.4-hour activity and longer components. After allowing one year for intermediate activities to die out, decay for a period of one year showed a one-year activity. When the activity due to this component was subtracted from the earlier data, the presence of an activity of approximately 43-day half-life was established. Subtraction of this in turn showed a 37-hour activity, indicating the presence of 4.4-hour Ru^{105} decaying to 37-hour Rh^{105}. The 43-day activity was presumed to be Ru^{103}.

Aluminum absorption measurements on the one-year activity showed the characteristic hard beta particle of the Rh^{106} daughter in equilibrium with 1.0-year Ru^{106}.

Palladium.—Two palladium activities were observed directly, 21-hour Pd^{112} and 14-hour Pd^{109}. The formation of 26-minute Pd^{111} was demonstrated by the separation of 7.5-day Ag^{111} from a portion of the target immediately after bombardment and from a second portion after an interval of three to four hours. The specific activity of Ag^{111} was significantly higher in the second portion than in the first, indicating its formation by the decay of Pd^{111}.

Decay was measured without absorber, through 80 mg/cm^2 of aluminum (to block the beta particles of Pd^{112}), and through 490 mg/cm^2 of aluminum (blocking the beta particles of Pd^{112} and Pd^{109}, but allowing the radiation of 3.2-hour Ag^{112} in equilibrium with Pd^{112} to be counted). Growth of the 3.2-hour Ag^{112} was observed.

Silver.—Decay measurements through 1380 mg/cm^2

aluminum (to block all particulate radiation from silver isotopes except that of Ag^{112}) showed the 3.2-hour Ag^{112}. Decay measurements without absorber on a sample separated very soon after bombardment (to minimize the effect of the growth of 3.2-hour Ag^{112} from 21-hour Pd^{112}) gave the best data on the 5.3-hour Ag^{113}. The 7.5-day Ag^{111} was clearly seen, and shown to be formed (see above) as a primary fission product, its independent yield being 18–20 percent of the total observed β^- chain. Decay followed over a period of ten months showed an activity of 250–270 days, presumably Ag^{110}.

The formation of 20-minute Ag^{115} was shown by separating 53-hour Cd^{115} from a portion of the target immediately after bombardment and from a second portion after an interval of about four hours. The specific activity of Cd^{115} separated from the second portion was significantly higher than that from the first portion, indicating its formation by decay of Ag^{115}.

A sample of silver was initially separated from cadmium, then allowed to decay. Cadmium separated from this sample after four hours showed a 53-hour half-life with no indication of a 43-day component. This indicates that Ag^{115} decays predominantly to the Cd^{115} ground state rather than to Cd^{115m}.

Aluminum absorption measurements on the 3.2-hour activity showed the presence of the characteristic 3.6-Mev beta particle of Ag^{112}. Measurements on the 7.5-day activity showed the 1-Mev beta energy of Ag^{111}. The background due to electromagnetic radiation was less than 0.05 percent of the initial activity. Correcting for the difference in counting efficiencies, this means that any 8.6-day Ag^{106} must be present in an amount less than 5 percent of that of Ag^{111}.

Cadmium.—Decay measurements through 946 mg/cm^2 of beryllium (to block all particles of energy less than 1.9 Mev) showed evidence of the 49-minute Cd^{111m} and indicated the possible presence of 6.7-hour Cd^{107}. Decay of the beta radiation showed 2.8-hour Cd^{117}, 53-hour Cd^{115}, and 43-day Cd^{115m}. There was a very long-lived component which suggested the presence of either 470-day Cd^{109} or 5-year Cd^{113m}. Aluminum absorption measurements showed the 1.1-Mev beta particle of the 53-hour Cd^{115}.

Tin.—Decay measurements showed components of about 27-hour and of 9.5-day half-lives and a longer component, presumably of 130-day half-life. These seem to be due to Sn^{121}, Sn^{125}, and Sn^{123}, respectively. The other isomer of each mass number was not observed.

Tellurium.—Of the many components in the tellurium decay curve, it was possible to resolve only the 30-hour Te^{131m} and its 8-day I^{131} granddaughter in the decay curve.

Cesium.—The predominant activity in the cesium fraction was the 13-day Cs^{136}. Aluminum absorption measurements on this activity showed the characteristic 0.3-Mev beta energy of Cs^{136}.

Barium.—Most of the bombardments were interrelated by measuring the amount of 12.8-day Ba^{140} produced and using this as an internal monitor. In most cases the barium was not separated from radium. In these cases, the radiation from the sample was measured through sufficient aluminum absorber to prevent any alpha particles emitted by radium or its daughters from reaching the counter tube. In addition to observing its half-life, we identified Ba^{140} by observing the growth of its 40-hour La^{140} daughter.

A sample of the radioactive barium was analyzed in the mass spectrograph.[36] The emulsion side of the collector plate was placed against the emulsion of a second plate and the radioactive species allowed to decay for a period of about two weeks. Lines on the second or "transfer" plate indicated radioactive barium isotopes of masses 131, 133, 135, and 140 in comparable yields.

An approximately 10-day activity was observed in a cesium sample separated from a purified barium sample some time after bombardment. Although Ba^{131} has approximately the same half-life and may be present in yields of the same order of magnitude as Ba^{140}, the counting rate due to the activity of Ba^{131}—Cs^{131} detected by the Geiger-Müller tube is less than one percent of that of an equal amount of Ba^{140}—La^{140} because of the large difference in counting efficiencies.

Components of 29 to 39 hours with soft particle radiation were observed in the decay curves. These probably represent a mixture of Ba^{133m} and Ba^{135m}. An 85-minute component, corresponding to Ba^{139}, was also observed. In a sample of barium separated from radium with an ion-exchange column, the 85-minute, 29- to 39-hour, and 12.8-day components were observed. The positrons of 2-hour Ba^{129} were not observed during a crude beta-ray spectrometer measurement of the column-separated barium.

Lanthanum.—Decay curves showed essentially a single component, the 40-hour La^{140}, over a period of 8 to 9 half-lives. Decay of the radiation which passed through 946 mg/cm^2 of beryllium (to block the particles and hence allow other possible electromagnetic radiation to show a more favorable counting efficiency relative to the radiation from La^{140}) showed a curve essentially parallel to the curve taken without absorber. Since the final separation of lanthanum was not accomplished until 56 hours after bombardment, the possibility of formation of nuclides of shorter half-life in comparable yield is not excluded.

Aluminum absorption curves of the 40-hour activity compared closely with known absorption curves of the radiations from the 40-hour negative beta particle emitting daughter of Ba^{140}. Through the use of the absorption curves, the counting rate was corrected for air and window absorption, and for the contribution of the electromagnetic radiation. The disintegration rate was calculated from this corrected counting rate.

[36] Mass spectrographic analysis by F. L. Reynolds of this laboratory.

Calculations based on the relative yields of Ba^{140}, La^{140}, and Nd^{140} (explained in Sec. V) show that approximately 30 percent of the total yield at mass number 140 is initially formed as La^{140}.

Cerium.—Decay curves showed components of approximately 35 hours and approximately 30 days with a component of intermediate half-life. Analysis of the data indicated the presence of Ce^{143} with Pr^{143} daughter, and Ce^{141}. Additional decay over a period of about six months indicated the presence of 275-day Ce^{144}.

Comparison of the number of x-rays emitted by the long-lived activity with the number from Ce^{144} tracer obtained from slow neutron fission of uranium indicated the presence of 140-day Ce^{139} in our sample. Aluminum absorption measurements on the long-lived component showed two beta components which could be attributed to Ce^{144} and the 17-minute Pr^{144} in equilibrium.

Praseodymium.—Observation of the decay through 406 mg/cm^2 of aluminum showed a 19-hour half-life. Observation of the decay without absorber showed two components, one of 13.5-day half-life, the second of half-life 16 to 19 hours. Aluminum absorption measurements on the 19-hour activity showed hard beta radiation of 2.3-Mev energy and indicated a soft component of about 0.6-Mev energy in about 20 percent abundance. After decay of the 19-hour activity, aluminum absorption measurements on the 13.5-day activity showed a particle of 0.92-Mev maximum energy. On the basis of the decay and absorption measurements, it was concluded that Pr^{142} and Pr^{143} were both present in good yield.

The Pr^{142} is a shielded nuclide; consequently, its independent yield was obtained directly. The independent yield of Pr^{143} was obtained as the result of an experiment in which the 33-hour Ce^{143} parent was removed from the rare earth group within two hours after bombardment. From the yield curve (Fig. 1) it is expected that the total yield of products of mass number 143 will be less than the total yield of products of mass number 142. Since in the case of these two isotopes the ratio of the yield of Pr^{143} to that of Pr^{142} was about 1.7, the Pr^{143} represents a greater fraction of the total yield at mass number 143 than the Pr^{142} does of its total mass number yield. This indicates that whereas the most probable primary atomic number for a given mass number corresponds to the neutron excess side for isotopes of the lighter elements, the trend is for the most probable primary product to be much closer to the region of beta stability for the higher mass chains.

Neodymium.—Observation of the decay through 407 mg/cm^2 of beryllium (sufficient to block the beta particles of Nd^{147}) showed two components. After subtraction of the gamma ray activity due to the 11-day Nd^{147}, a 3.3-day decay was found. This corresponds to Nd^{140}. Decay measurements without absorber showed the 11-day half-life of Nd^{147} for over three half-lives. Aluminum absorption curves showed the characteristic beta particle energy of Nd^{147}. Since less than 2 percent of the initial total activity could be attributed to Nd^{140}, this activity did not interfere and was not characterized by absorption measurements. Its counting efficiency was calculated from the data of Wilkinson and Hicks.[37]

Calculations based on the relative yields of Ba^{140}, La^{140}, and Nd^{140} show that approximately 7.4 percent of the total yield at mass number 140 is due to Nd^{140}.

Promethium.—Decay was observed both without absorber and through 485 mg/cm^2 of aluminum. The decay as observed without absorber showed components with half-lives of about 13 hours, about 47 hours and 43 days. The first component is as yet unidentified, although an activity with such a half-life has been reported[38] to be formed by deuteron bombardment of neodymium. The other two components correspond to Pm^{149}, for which several half-lives between 47 and 55 hours have been reported, and to one of the two isomers of Pm^{148}. Crude beta-ray spectrometer measurements on the long-lived species show two resolvable beta components, one of about 600 kev and the other of about 2.4 Mev, the second component being about 5–10 percent as abundant as the first. This leads us to believe that the 43-day species corresponds to the upper state of Pm^{148}, since the 2.4-Mev radiation could arise from an unobserved isomeric transition leading to a small equilibrium amount of 5.3-day Pm^{148} ($\sim$2.5 Mev β^-). Absorption of the electromagnetic radiations of the 43-day component in copper showed no detectable neodymium x-rays.

Decay measurements through absorber showed all three of the above components and, in addition, the 5.3-day Pm^{148}.

Samarium.—The samarium decay showed components of about 10 hours and of 47 hours, the 47-hour component being quite prominent. After decay of this activity, a 15- to 16-day line was observed. Aluminum absorption measurements on the 47-hour activity indicated a beta particle of about 0.8-Mev energy. The 2.4-Mev beta particle of Eu^{156} was also observed in the absorption measurements.

The principal activities found in the samarium fraction were thus the 47-hour Sm^{153} and the 10-hour Sm^{156} with its 15.4-day Eu^{156} daughter. The yield of Sm^{156} relative to Sm^{153} was about 27 percent. The yield of Sm^{153} represents the entire beta decay chain for mass 153 whereas Eu^{156} is expected to be a large contributor to the yield of mass number 156.

Europium.—The principal europium activity was the 15.4-day Eu^{156}. Aluminum absorption measurements showed the characteristic 2.4-Mev beta particle of Eu^{156}.

Terbium.—The terbium decay curve could be resolved roughly into two components, the longer of which had a half-life of 74 days. The shorter component

[37] G. Wilkinson, and H. G. Hicks, Phys. Rev. 75, 1687 (1949).
[38] M. L. Pool and L. L. Quill, Phys. Rev. **53**, 437 (1938).

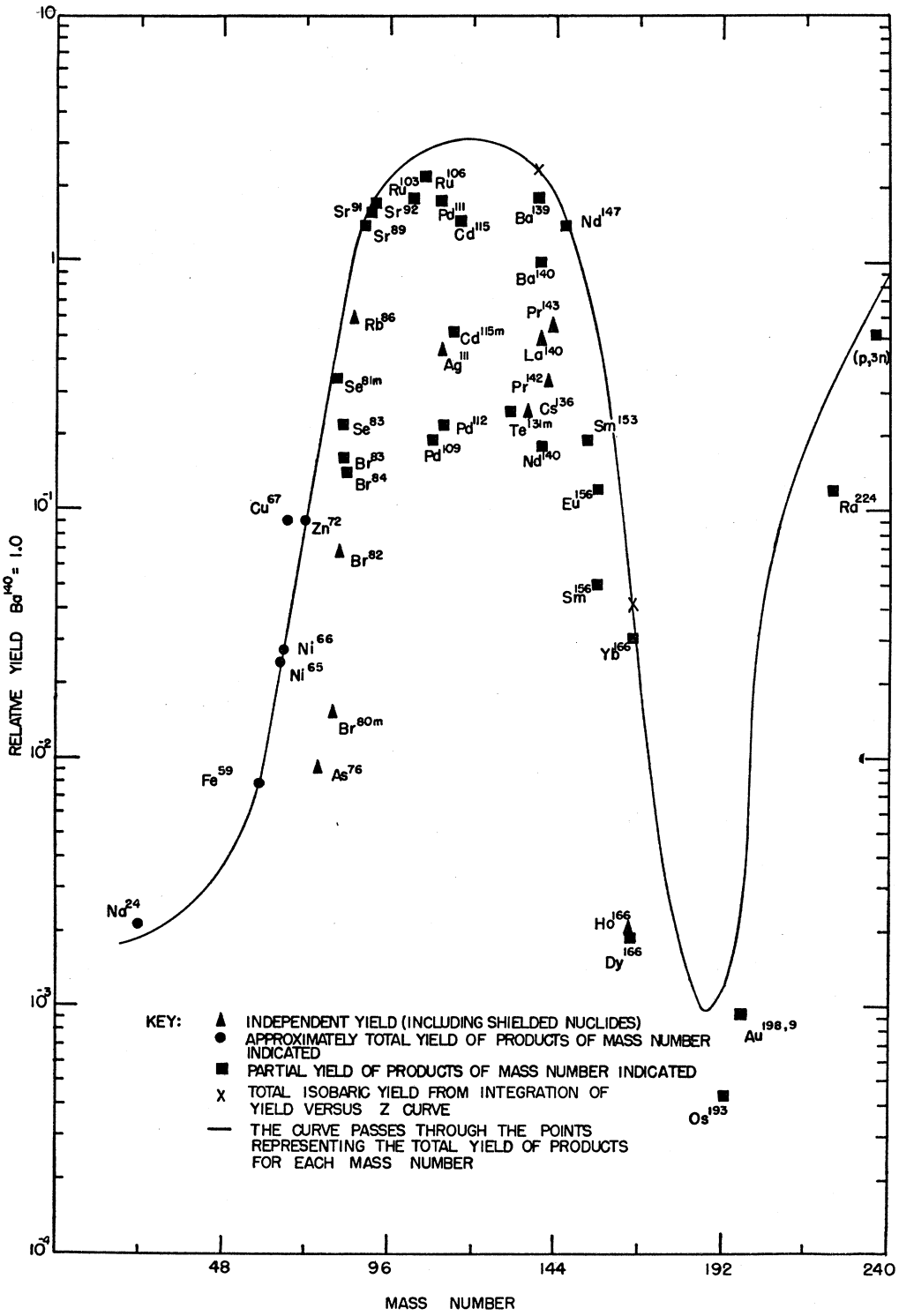

FIG. 1. Yields of the various observed species (relative to Ba^{140}) plotted as a function of mass number.

was due to a mixture of activities with half-lives between 5 and 7 days and a shorter one. Decay was observed without the use of absorber and also through 183 mg/cm² of beryllium (sufficient to block the 0.5-Mev beta particles of Tb^{161}). After subtraction of the activity due to the 74-day residuum, the decay measurement taken through beryllium showed strong indication of a 5.1-day activity. The decay observed without the

use of absorber showed a mixed activity with a 6.8-day activity predominating after subtraction of the activity due to the 74-day component. These observations indicate the formation of Tb^{160} and Tb^{161}, and the probable formation of Tb^{153} and Tb^{156}.

In the terbium fractions separated 12 to 14 hours after bombardment, traces of alpha activity were observed. A sample submitted to Dr. J. O. Rasmussen for alpha pulse analysis showed alpha energy and decay corresponding to 4.1-hour Tb^{149}.

Dysprosium.—The chief component observed in the dysprosium decay was the 80-hour Dy^{166}. A long-lived activity was also observed, but it was not possible to determine its half-life. Aluminum absorption measurements on the equilibrium mixture showed the 0.4-Mev beta particle of Dy^{166} and the 1.9-Mev beta particle of the Ho^{166} daughter.

Calculations based on the relative yields of Dy^{166}, Ho^{166}, and Yb^{166} (see Sec. V) indicate that 2.54 percent of the total yield at mass number 166 is formed as Dy^{166}.

Holmium.—The major component observed in the holmium decay was due to the 27-hour Ho^{166}. The decay was measured through eight half-lives. The activity remaining as a long-lived component corresponded to less than 0.02 percent of the Ho^{166} activity present at the end of the bombardment. Aluminum absorption measurements showed the approximately 1.9-Mev beta energy of Ho^{166}. The 7-day activity presently assigned to Ho^{163} was not observed in our holmium sample in a resolvable amount.

Calculations based on the relative yields of Dy^{166}, Ho^{166}, and Yb^{166} indicate that 4.7 percent of the total yield at mass number 166 is due to Ho^{166}.

Erbium.—Decay of the erbium fraction could be resolved into at least three components, one of which gave rise to a holmium daughter of about 4.5 hours half-life. Half-lives of the three components were 9.4 days (Er^{169}), 72 hours (unknown) and a shorter component with an apparent half-life of 12 to 24 hours. Aluminum absorption measurements showed that the 72-hour component was associated with 1.3-Mev electrons (either positive or negative), while the shortest-lived component decayed primarily by gamma-ray emission. Nervik and Seaborg[12] have identified a 29-hour Er^{160} which decays to a 5.0-hour Ho^{160}, the mass assignment being verified by mass spectrometric separation. Ten-hour Er^{165} is expected to be present also, so it is felt that the short-lived component represents a mixture of Er^{160} and Er^{165}. The 72-hour component represents a previously unreported activity. On the basis of its counting yield relative to Er^{169} we expect it to be a negatron active isotope of erbium with mass number 169 or greater. The possibility of an independently-decaying isomer of Er^{169} is not eliminated. Decay measurements on the erbium fraction taken through 99.7 mg/cm^2 of beryllium (to eliminate the activity of Er^{169}) showed that the initial activity due to the 72-hour component was approximately equal to that of Er^{169} while the initial activity of the short-lived component was ten times as great. This indicates (considering relative counting efficiencies) that the yield of neutron-deficient erbium isotopes is considerably greater than the yield of neutron-rich isotopes.

Thulium.—Decay measurements on the thulium fraction could not be resolved into separate components unambiguously. Strong indications were seen of the presence of 9.6-day Tm^{167} and of a shorter-lived component with possible growth of a daughter activity, which could be 29-hour Tm^{165} giving rise to 10.2-hour Er^{165} as characterized by Nervik and Seaborg,[12] together with 7.7-hour Tm^{166} which is known to be present as the result of the observation of its growth from its Yb^{166} parent. The later portions of the decay curve seemed to indicate the presence of a very long-lived activity, which could be due to Tm^{168}, Tm^{170}, Tm^{171} or a mixture.

Ytterbium.—Decay of the ytterbium sample showed two prominent components, the 32.5-day Yb^{169} and a component of 66-hour apparent half-life. Growth of a 7.7-hour component, chemically identified as thulium, is due to Tm^{166} as mentioned above. The shorter-lived ytterbium activity is therefore presumed to be due to Yb^{166}. Decay measurements taken through 183 mg/cm^2 of beryllium absorber showed the same components, but the half-life of the shorter-lived component was reduced to 60 hours. Nervik and Seaborg[12] have reported the half-life of Yb^{166} to be 53.8 hours. We presume that the discrepancy in half-life indicates the presence of a small amount of Yb^{175} (4.2 days) whose radiations would be discriminated against as a result of the presence of the absorber.

Spallation products.—The work of O'Connor and Seaborg[9] on the bombardment of uranium with 380-Mev helium ions showed that there was apparently a continuous yield of radioactive products for the entire range of elements from the uranium region down to the vicinity of atomic number 25, the lowest atomic number for which they attempted to determine a yield. Above mass number about 120, the yield of fission products decreased with increasing atomic number. In the region above mass number about 200 the yield curve was observed to increase with increasing mass number. This increase was attributed to products formed by high energy spallation of uranium. The yield of products found in the region of the minimum of the curve might be attributed to a combination of fission products and spallation products. That fission can occur in such a manner as to give products of such high mass was shown by the detection of product nuclei of correspondingly low mass.

In the present work it was observed that the primary fission products tend toward the neutron-deficient side of stability with increasing mass number in the region 130 to 170. In the region of mass number 180 to 200, however, several negatron-emitting nuclides were

observed which we have attributed tentatively to spallation reactions.

IV. TABULATION OF OBSERVED YIELDS

The relative yield values, Y_R, (Ba^{140} taken to be 1.00) are given in Table I and are plotted in Fig. 1. These were calculated from the measured counting rates for the listed nuclides, whose identification was described in the previous section, taking into account the various factors described in Sec. II. The curve in Fig. 1 is drawn so as to represent the total isobaric yield at each mass number with this total yield estimated as described in Sec. V.

Since it was thought desirable to establish the relationship between these relative yields and the corresponding absolute yields (cross sections) some of these yields (which include the precursors) were redetermined in experiments where direct comparisons with the known yield of the reaction[39] $Al^{27}(p,n3p)Na^{24}$ could be made. These cross sections are listed in Table II together with the corresponding relative yields (from Table I).

TABLE I. Yields of observed fission and spallation products relative to Ba^{140}.

Mass number	Nuclide measured	Class[a]	Y_R
24	Na^{24}	2	0.0021
59	Fe^{59}	2	0.0078
65	Ni^{65}	2	0.024
66	Ni^{66}	2	0.027
67	Cu^{67}	2	0.091
72	Zn^{72}	2	0.090
76	As^{76}	1	0.0091
80	Br^{80m}	1	0.015
81	Se^{81m}	3	0.32
82	Br^{82}	1	0.067
83	Se^{83}	3	0.22
	Br^{83}	3	0.16
84	Br^{84}	3	0.14
86	Rb^{86}	1	0.59
89	Sr^{89}	3	1.5
91	Sr^{91}	3	1.6
92	Sr^{92}	3	1.7
103	Ru^{103}	3	1.8
106	Ru^{106}	3	2.2
109	Pd^{109}	3	0.19
111	Pd^{111}	3	1.6_5
	Ag^{111}	3	0.4_1
112	Pd^{112}	3	0.22
115	Cd^{115}	3	1.4_6
	Cd^{115m}	3	0.51
131	Te^{131m}	3	0.25
136	Cs^{136}	1	0.25
139	Ba^{139}	3	1.8
140	Ba^{140}	3	1.00
	La^{140}	1	0.48
	Nd^{140}	3	0.18
142	Pr^{142}	1	0.33
143	Pr^{143}	1	0.55
147	Nd^{147}	3	1.4
153	Sm^{153}	3	0.19
156	Sm^{156}	3	0.05
	Eu^{156}	3	0.12
166	Dy^{166}	3	0.0019
	Ho^{166}	1	0.0020
	Yb^{166}	3	0.030
193	Os^{193}	3	0.00043
~198	$Au^{198,199}$	3	0.00094
224	Ra^{224}	3	0.12
236	Np^{236} [b]		0.51

[a] Class 1, independent yield or shielded nuclide; Class 2, approximately total yield of mass number; Class 3, partial yield of mass number.
[b] Meinke, Wick, and Seaborg (unpublished).

TABLE II. Cross sections for formation of certain observed fission products.

Nuclide	σ_f(mb)	Y_R (Ba^{140} = 1.00)
Cu^{67}	2.1	0.09
Se^{81m}	7.5	0.32
Sr^{89}	35	1.5
Ag^{111}	$48._5$	2.1
Cd^{115}	$33._6$	1.4
Cd^{115m}	12	0.51
Ba^{140}	$23._5$	1.0

TABLE III. Yields of nuclides along certain isobaric chains.

Mass number	Nuclide measured	Relative yield (Ba^{140} = 1.00)	Estimated fraction of total chain
83	Se^{83}	0.22	0.45
	Br^{83}	0.16	0.33
111	Pd^{111}	1.6_5	0.5
	Ag^{111}	0.4_1	0.08
140	Ba^{140}	1.00	0.43
	La^{140}	0.48	0.21
	Nd^{140}	0.18	0.075
166	Dy^{166}	0.0019	0.044
	Ho^{166}	0.0020	0.047
	Yb^{166}	0.030	0.72

Integration of the yield *versus* mass number curve (Fig. 1) in terms of the cross sections for the formation of the fission products indicates a total fission cross section of 2.0 barns for uranium irradiated with 340- to 350-Mev protons. A single direct measurement[40] with an ionization chamber for the same reaction yielded a definitely lower value, somewhat less than a barn.

V. ISOBARIC YIELD STUDIES

Identification of the charge of the fissioning nucleus depends on the determination of the primary fission products. Experimentally we have attempted to measure the independent yields of various members of several reference mass number chains. The nuclide whose yield is represented by the maximum of the curve obtained by plotting the independent yield as a function of atomic number for a given mass number is defined to be the "primary" product for that mass number. In practice it is usually quite difficult experimentally to measure directly the independent yields for many of the members of a given mass number chain. Those independent yields which have been measured experimentally are listed in Table III. The yields of the measured members farthest from beta stability for any chain included the yields of their precursors.

In order to interpret the data obtained for independent yields we have assumed that the independent

[39] Stevenson, Hicks, and Folger (to be published).
[40] J. Jungerman, Phys. Rev. **79**, 632 (1950).

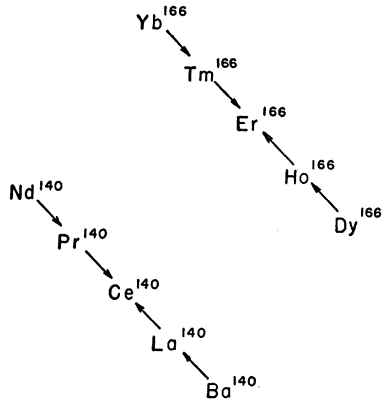

FIG. 2. Genetic relationships of the mass number 140 and mass number 166 decay chains.

yields of the various isobars of a given decay chain are distributed symmetrically about some particular Z in a manner which can be well approximated by the normal curve of error, using suitable parameters to adjust the half-width and peak height of such a distribution curve to the experimental results obtained. A description of the mathematical method of fitting the normal curve of error to such data is given in the Appendix.

It will be seen from the Appendix that three experimental data are sufficient to establish the constants of the curve. One eventually, therefore, could obtain some idea of the validity of our basic assumption by studying the independent yields in chains containing more than three members. Suitable chains are those of mass numbers 166, 141, 111, and 72, each chain containing four measurable members. Initial sets of three experimental data, as shown in Table III, have been obtained for the chains of mass number 140 and mass number 166. The genetic relationship of these chains is shown in Fig. 2.

Figures 3 and 4 show the standard curve of error histograms for the mass number 140 and mass number 166 chains, respectively. The parameters for these curves are tabulated in Table IV.

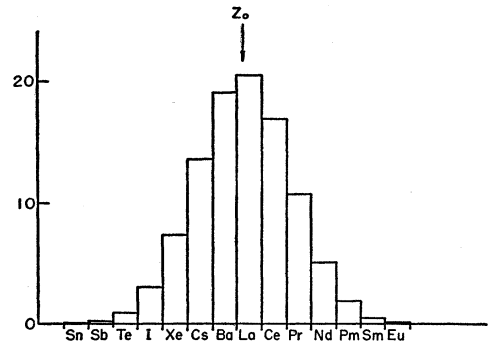

FIG. 3. Relative direct yields of fission products of mass number 140.

It is apparent that if we could predict the parameters of these charge-distribution histograms as functions of the chain mass number, we could derive factors for each mass number to give the total chain yield, including stable nuclides, in terms of the yield of any nuclide of the chain. The rough estimates of the fractions of total chain yields given in Table III were made in this manner on the basis of the few data presently available.

VI. DISCUSSION

Examination of the data presented here shows a few marked trends. Almost all of the low atomic number nuclides which were identified are of the neutron-excess type. As higher atomic numbers are approached, neutron-deficient nuclides increase in relative abundance of formation. In the ytterbium fraction, almost all the activity is due to neutron-deficient nuclides. In the spallation region which merges with the heavy fission fragments in the region of mass number 180, however, neutron-excess nuclides again are observed (in the elements osmium, gold, and radium). There seems to be a rather well defined region of fission products in the mass number range of the single hump in Fig. 1, and a region of spallation products in the region of the ascending curve starting around mass number 190, with a pronounced minimum in the yield curve between these two regions, presumably representing products from both fission and spallation reactions.

The yield *versus* mass number curve appears to be roughly symmetrical about mass number 114, indicating a "most probable fissioning nucleus" of mass number about 228. The data on independent yields can also be used to derive information concerning the nature of the fissioning nucleus, or, as it turns out, about the spread in mass number of the fissioning nuclei.

In a test of the possible extension to uranium of the hypothesis of Goeckermann and Perlman[2] that in high-energy fission of bismuth the most probable primary fission products are those with the same charge-to-mass ratio as the fissioning nucleus, we can take our value for Z/A of the "primary" fission products and calculate the mass of the "most probable fissioning nucleus" assuming various reasonable values for its

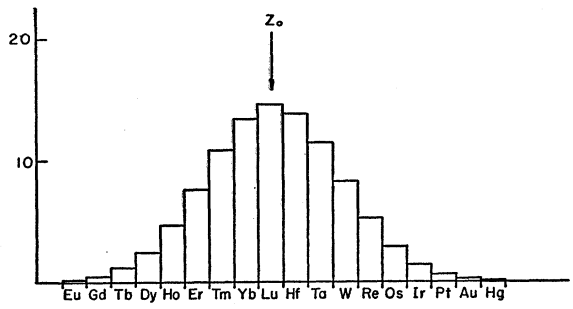

FIG. 4. Relative direct yields of fission products of mass number 166.

Z. The results (based on our best experimental value for Z/A of 0.42 from the mass number 140 and 166 chains) are listed in Table V.

It will be seen that this method leads to a maximum value of 221 for the mass number of the most probable fissioning nucleus, which is not in agreement with the value 228 as deduced above from mass-yield data. The maximum value of 221, moreover, can be attained only by a rather unlikely reaction mechanism. When we consider the probable sources of error in the mass-yield measurements the agreement is worse, since the yields on the heavy-mass side of the curve are most likely to pass unobserved because of direct formation of stable or neutron-deficient nuclides. Consequently we expect the observed location of the peak at mass number 114 to be, if anything, too low.

The different results from the two methods of arriving at a "most probable fissioning nucleus" are apparently due at least in part to the fact that any postulate of the existence of such a nucleus (or small range of nuclei) is not a good approximation in the high energy fission of uranium. It is reasonable to expect that uranium nuclei bombarded with 340-Mev protons will be left in widely different states of internal excitation; further, that even those which are left in roughly the same state of excitation will de-excite before fission by several different modes, leading (among other results) to different numbers of nucleons evaporated. This suggests that the observed fission yield curve is the result, not of a small number of fissioning species, but of a group of fissioning species whose relative importance is distributed in a manner dependent upon the bombarding energy and the bombarding particle, in agreement with the deductions of Douthett and Templeton.[14] The spread in mass number of the nuclei which undergo fission will be much broader than in the case of the high-energy fission of bismuth because in the case of uranium all of the spallation product nuclei formed by the emission of any number of neutrons (and a few protons) have relatively low potential barriers against fission. In the case of bismuth a most probable fissioning nucleus is better defined because the emission of a certain number of neutrons is necessary in order to lower the potential barrier to a point where fission is relatively probable and the emission of any protons leads to nuclei for which fission is relatively improbable. In addition, the greater possibility of fission for nuclei

TABLE IV. Measured constants of the mass number 140 and mass number 166 chains.

	Z_0	Standard deviation	Z_0/A
mass 140	57	2.7	0.41
mass 166	71	3.9	0.43

TABLE V. Nature of the fissioning nucleus deduced from charge-to-mass ratio.

Z	A	$\Delta A = 238 - A$
93	221	17
92	219	19
91	217	21
90	214	24
89	212	26

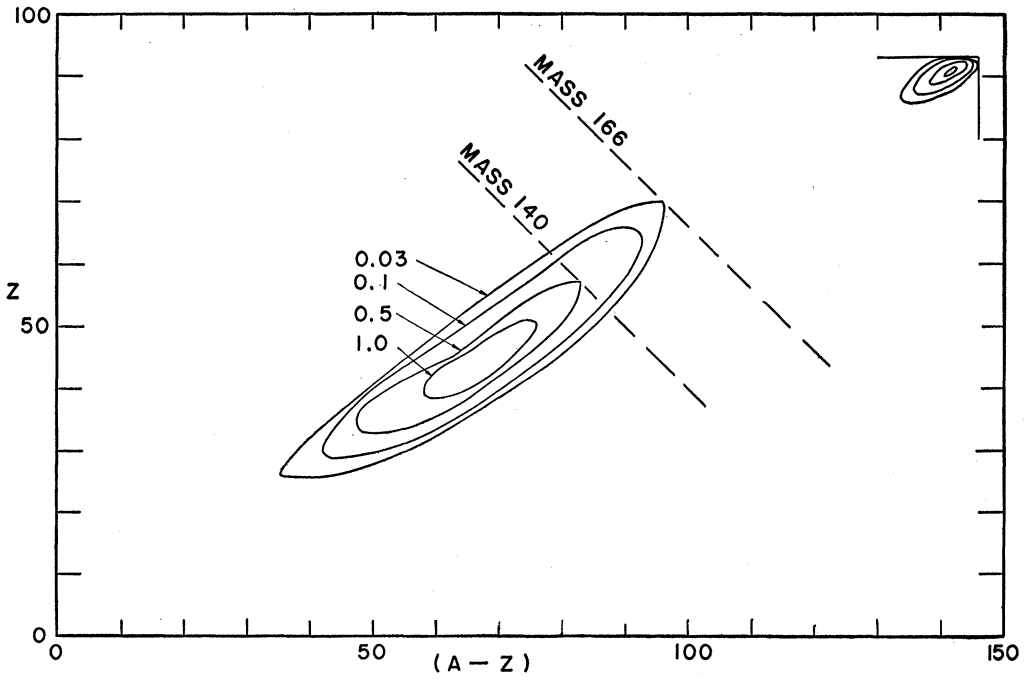

FIG. 5. Distribution of fission events and direct fission products in Z and $A-Z$ (schematic only).

with low excitation in the case of uranium means that a number of these nuclei may have a longer time to undergo the fission reaction which may permit more internal rearrangement of nucleons during fission.

Let us consider a nuclide formed by high-energy spallation of a U^{238} nucleus, this nuclide having an amount of internal energy much in excess of the fission potential barrier. This energy may be dissipated in one of three different ways: it may be used to cause fission; it may be dissipated as radiation or particle emission, the final nuclide descending to a nonfissioning ground state; or it may be carried off, in part or entirely, by an emitted neutron, proton, or composite particle, leading to a different nuclide which again may undergo one of these three changes. If we represent all the possible spallation product nuclides as points on a plane with coordinate axes Z and $A-Z$, then the various spallation and fission products possible from U^{238} bombarded with protons will all fall within the quadrant of this plane having $Z<93$, $A-Z<146$. The relative numbers of fission events occurring in various heavy nuclei lying within the spallation region can be described by a contour map. The contour lines are loci of points of equal numbers of fission events. The fission fragment yield curve may be plotted in the same way on the same chart (see Fig. 5). A dotted line of slope -1 represents an isobaric chain. The independent yield of the members of this chain as a function of Z is given by the value represented by the contour line intersected for each Z.

We may assume that the shape of the fissioning-nucleus contour map is markedly energy-sensitive. Factors influencing this shape will include the abundance of excited nuclei of various A and Z, their degree of excitation (which, presumably, is different for different A and Z and which is, also, probably not unique for any given A and Z) and the probability of fission for a nucleus of each particular A and Z under the given conditions of excitation. Let us further assume that the fission-fragment yield distribution is uniquely determined by the fissioning nucleus distribution. Some qualitative predictions of the behavior of the fission-fragment yield curve with variation of bombarding energy may then be made.

The most obvious effect of increasing the bombardment energy will be to increase the spread of the distribution of the spallation products leading to fission, since Douthett and Templeton[14] have shown that excess bombarding energy does not appear as kinetic energy of the fragments. This will lead to a lower average mass number for the "fissioning nucleus," with its concurrent effect of lowering the mass number of the maximum yield of fission fragments. Also, should neutrons be evaporated from the excited pre-fissioning nuclides in preference to protons or other charged particles in sufficient degree, as seems likely, the charge-to-mass ratio of the average fissioning nucleus, and hence of its fragments, should be increased. We thus expect that at high energies nuclides closer to beta stability, or even on the neutron deficient side, should appear in greater relative abundance, as is actually observed.

VII. ACKNOWLEDGMENTS

We wish to express our gratitude to Professors I. Perlman and L. Malatesta, Drs. H. G. Hicks, J. Miller, B. C. Haldar, G. Higgins, W. Nervik, and G. Rudstam and Major W. Worthington for helpful discussion and experimental assistance. We wish also to thank J. Conway and M. Moore for providing many spectrographic analyses of materials used, J. T. Vale, Lloyd Hauser, and the crew of the 184-in. cyclotron for their cooperation in irradiating our targets, and Mrs. Elinor Potter and Mrs. Roberta Garrett for their valuable assistance in the counting of samples. One of us (P. C. Stevenson) wishes to thank the National Research Council for a U. S. Atomic Energy Commission Postdoctoral Fellowship in the Physical Sciences. This work was performed under the auspices of the U. S. Atomic Energy Commission.

APPENDIX. DERIVATION OF THE CHARGE DISTRIBUTION OF ISOBARIC PRIMARY FISSION FRAGMENTS FROM CHAIN YIELD DATA

1. Let us assume that the independent fission yields of the fission fragments of a given mass are distributed according to a normal curve of error.

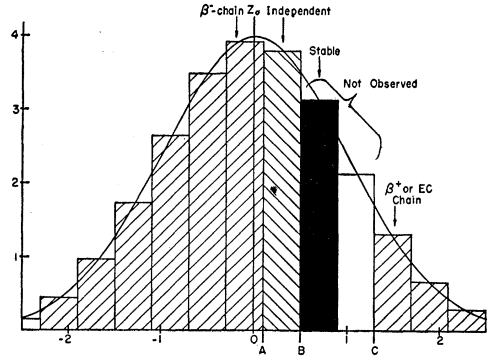

FIG. 6. Histogram fitted to the normal curve of error. [Ordinate, relative amounts; Abscissa, $(Z-Z_0)/\delta$.]

TABLE VI. Values of B and δ from the $Ba^{140}/(Ba^{140}+La^{140})$ ratio.

$\alpha=\delta$	$u=B$	$\alpha=\delta$	$u=B$
0.10	−1.66	0.60	+0.74
0.15	−0.89	0.70	+0.90
0.20	−0.47	0.80	+1.04
0.25	−0.19	0.90	+1.17
0.30	+0.02	1.00	+1.29
0.35	+0.20	1.20	+1.50
0.40	+0.34	1.40	+1.71
0.45	+0.46	1.60	+1.92
0.50	+0.56		

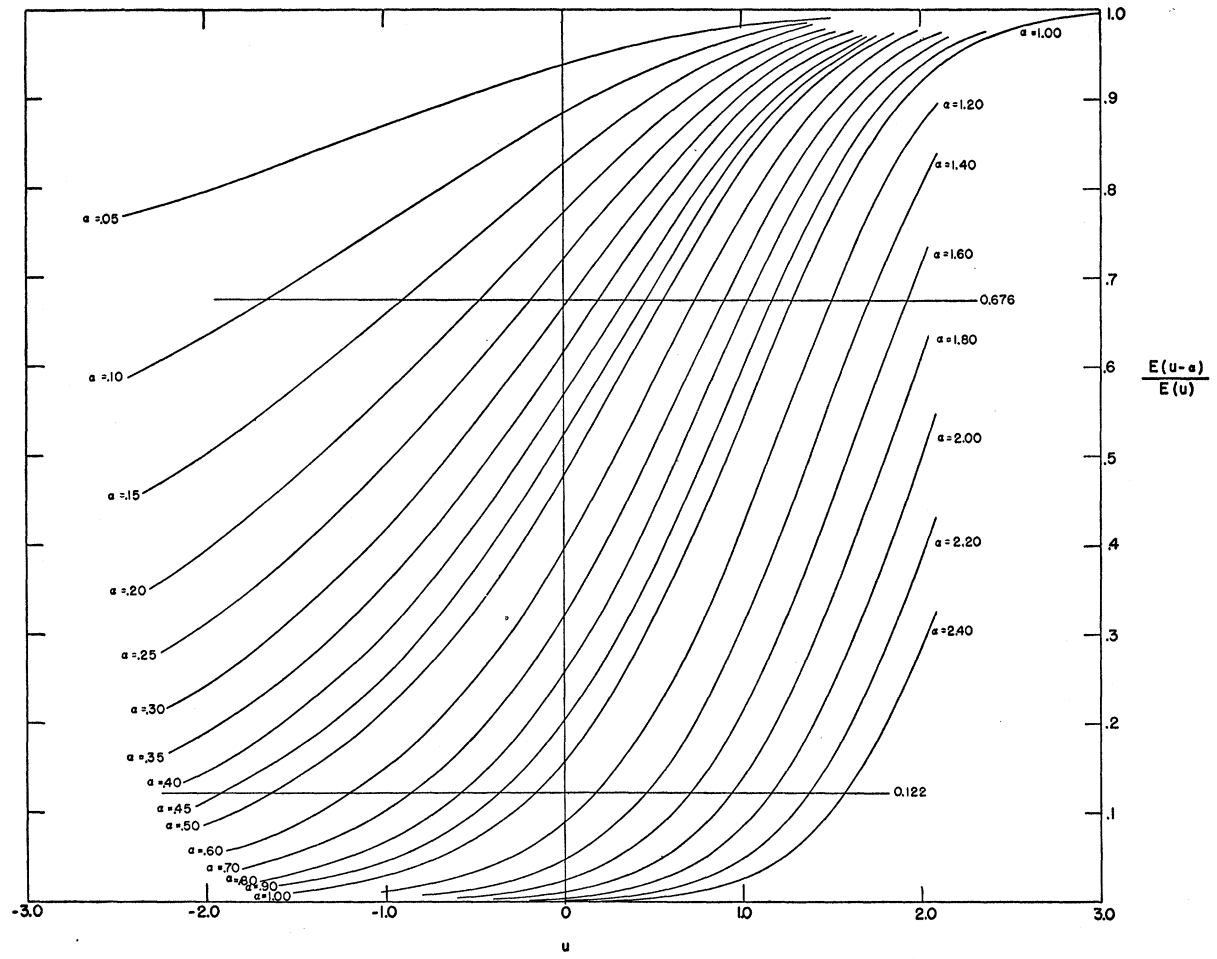

FIG. 7. $[E(u-\alpha)]/[E(u)]$ plotted as a function of u for various α.

2. Let us consider a normal curve of error fitted to a histogram, as shown in Fig. 6. Let the standard deviation of the normal curve of error be unity and the width of each block of the histogram be δ.

3. Let us consider data of the form obtained in our experiments. The yields observed for observable nuclides furthest from stability (on each side of stability) include all the yields from isobars still further from stability. Let species "A" be a β^- active nuclide with precursors too short to separate chemically; let species "B" be the (unstable) decay product of "A"; let species "C" be an isobaric neutron-deficient species which is chemically observable and has short precursors. Let us assume that the independent yield of "B" is measurable.

TABLE VII. Values of B and δ from the $Nd^{140}/(Ba^{140}+La^{140})$ ratio.

α	$u=B$	$\delta=\frac{1}{2}\alpha-u$	α	$u=B$	$\delta=\frac{1}{2}\alpha-u$
0.45	−1.92	+2.15	1.20	+0.17	+0.43
0.50	−1.64	+1.89	1.40	+0.46	+0.25
0.60	−1.21	+1.51	1.60	+0.70	+0.09
0.70	−0.87	+1.21	1.80	+0.93	−0.03
0.80	−0.58	+0.98	2.00	+1.16	−0.16
0.90	−0.32	+0.77	2.20	+1.37	−0.26
1.00	−0.16	+0.66	2.40	+1.57	−0.37

4. Let σ_A be the yield of A, σ_B be the yield of B, and σ_C be the yield of C, and let Σ be the yield of the total isobaric chain.

5. Let

$$E(x)=\int_{-\infty}^{x}\operatorname{erf}(t)dt.$$

Then

$$\sigma_A=E(A)\cdot\Sigma,$$
$$\sigma_A+\sigma_B=E(B)\cdot\Sigma,$$
$$\sigma_C=E(-C)\cdot\Sigma.$$

6. Now if the block width is δ, then $A=B-\delta$ and $C=B+n\delta$, where n is the number of intervening unobservable species (shown as two in the figure).

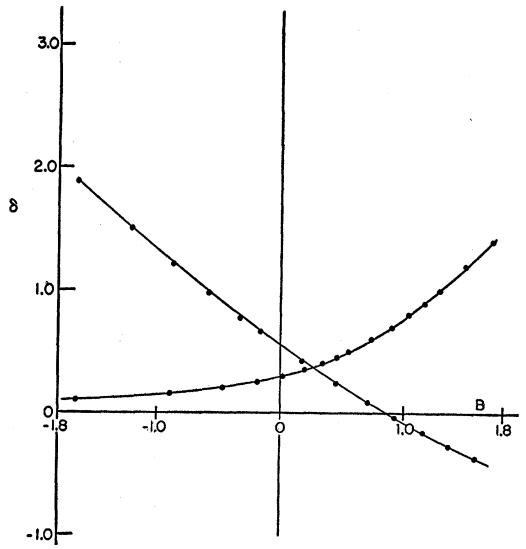

FIG. 8. Graphical solution for δ and B (mass number 140).

Therefore,

$$7.\qquad \frac{\sigma_A}{\sigma_A+\sigma_B}=\frac{E(B-\delta)}{E(B)},$$

$$8.\qquad \frac{\sigma_C}{\sigma_A+\sigma_B}=\frac{E[B-(2B+n\delta)]}{E(B)}.$$

9. Figure 7 shows a plot of $[E(u-\alpha)]/[E(u)]$ as a function of u for various α. By selecting a particular value for this fraction, which is analogous to the expressions in steps 7 and 8, we get α as a function of u. In the cases of the expressions in steps 7 and 8, we get δ as a function of B from step 7, and $2B+n\delta$ as a function of B from step 8 which gives δ as a second function of B. This is equivalent to two simultaneous equations in δ and B, which can readily be solved graphically. The standard deviation of the histogram in units of atomic number is then $1/\delta$ and the charge Z_0 for maximum yield is $Z_B+\frac{1}{2}-B/\delta$ (the term $+\frac{1}{2}$ is included to compensate for the fact that the atomic number corresponding to species B is presumed to be represented in the center of the histogram block rather than at the righthand edge). Example 1: Let us consider the data for the mass number 140 chain as given in Table III. Here, since Ce^{140} (stable) and Pr^{140} (half-life 3.4 minutes) are not observable, $n=2$.

$$\frac{\sigma(Ba^{140})}{\sigma(Ba^{140})+\sigma(La^{140})}=0.676.$$

From Fig. 7, we get the values in Table VI, and

$$\frac{\sigma(Nd^{140})}{\sigma(Ba^{140})+\sigma(La^{140})}=0.122,$$

which in conjunction with Fig. 7 gives us the values in Table VII. The values of δ and B from Tables VI and VII are plotted in Fig. 8, which gives for a common solution $B=0.265$, $\delta=0.370$; or $Z_0=56.8$, $\delta=2.70$.